Oxygen deficiency defects in amorphous Al_2O_3

T. V. Perevalov,[1] O. E. Tereshenko,[1] V. A. Gritsenko,[1] V. A. Pustovarov,[2] A. P. Yelisseyev,[3] Chanjin Park,[4] Jeong Hee Han,[4] and Choongman Lee[4]
[1]*Institute of Semiconductor Physics, 13/Lavrentiev Avenue, 630090 Novosibirsk, Russia*
[2]*Ural State Technical University, 19/Mira Street, 620002 Ekaterinburg, Russia*
[3]*Institute of Geology and Mineralogy, 3/Koptyug Avenue, 630090 Novosibirsk, Russia*
[4]*Memory Division, Semiconductor Business, Samsung Electronics Co. Ltd., Yongin-si 449-712, South Korea*

(Received 5 April 2010; accepted 12 May 2010; published online 1 July 2010)

In the electron energy loss spectra for amorphous, atomic layer deposited (ALD) Al_2O_3 film, a peak at 6.4 eV was observed. First principle quantum chemical simulation shows that it relates to excitation of neutral oxygen vacancy in Al_2O_3. The 2.91 eV luminescence excited in a band near 6.0 eV in amorphous Al_2O_3 is similar to that in bulk crystals which is associated with neutral oxygen vacancy. Thus, the amorphous ALD Al_2O_3 film is oxygen deficient and the oxygen vacancy parameters are similar in crystalline and amorphous Al_2O_3. © *2010 American Institute of Physics*. [doi:10.1063/1.3455843]

I. INTRODUCTION

The interest in studying point defects in crystalline α-Al_2O_3 (corundum, sapphire) is due to its application in lasers, nuclear reactors, dosimeters, and its use as a substrate for the growth of semiconductors such as Si, GaN *et al.* The most best studied defect in corundum is the neutral oxygen vacancy (F-center).[1–8] Today amorphous Al_2O_3 films with high dielectric permittivity ($\varepsilon=10$) are regarded also as a promising gate dielectric for the metal-oxide-semiconductor transistor instead of SiO_2 ($\varepsilon=3.9$) (Refs. 9 and 10) and as a blocking dielectric for flash memory cells of new generation.[11,12] Now $TaN-Al_2O_3-Si_3N_4-SiO_2-Si$ (TANOS) structures are intensively investigated to develop the flash memory devices of gigabit and terabit scale. Information in such memory cells is stored as a charge accumulated in the electron and hole traps in Si_3N_4. The charge retention time should be at least ten years at 85 °C. Charge in the TANOS structure can flow along the electron traps in amorphous Al_2O_3 (Ref. 13) and a strong leakage current is the reason which limits its application in semiconductor devices. The identification of defects nature in amorphous Al_2O_3 is of great scientific and practical interest. Synchrotron radiation (SR), providing intense and broad spectral emission over the ultraviolet region, is a powerful tool for spectroscopic study of wide-band gap materials, particular crystalline and amorphous SiO_2.[14–16] Since amorphous Al_2O_3 is synthesized in thermodynamically nonequilibrium conditions, its atomic structure depends on the synthesis technique. In this work, the electron energy loss (EEL) and SR excited photoluminescence (PL) spectroscopy as well as the first principle theoretical investigation of electronic and atomic structure were used to study point defects, which are responsible for optical transitions and electron localization/transport in amorphous Al_2O_3 obtained by the atomic layer deposition (ALD) method.

II. EXPERIMENTAL

The amorphous Al_2O_3 films, approximately 20 nm thick, were synthesized by the ALD method from trimethylaluminum $Al(CH_3)_3$ and water vapor. The p-type silicon wafers of the (100) orientation and $\approx 10\ \Omega$ cm resistance were used as a substrate. EEL spectra (EELS) were measured using an electron spectrometer ADES-500 (Vacuum Generator) in reflection geometry, at the incidence angle of 55° and at incident electron energy of E=50 eV with angular resolution of 1°. The pressure in the analytical chamber was of about 10^{-11} torr.

PL and PL excitation (PLE) spectra were measured at 7.5 K both in stationary and time-resolved regimes using SR on a SUPERLUM station of the DESYLAB laboratory (Hamburg, Germany) .[17] The time delay (δt) relative to the excitation pulse and the time window length (Δt) were chosen taking into account the luminescence kinetics. Two time windows were used: with $\delta t_1=2.7$ ns, $\Delta t_1=11.8$ ns for the fast component and $\delta t_2=60$ ns, $\Delta t_2=92$ ns for the slow one. The PLE spectra were measured at excitation energy $E_{ex}=4-40$ eV and normalized to an equal number of incident photons using the sodium salicylate, the quantum efficiency of which does not depend on photon energy at $h\nu>3.7$ eV.

III. RESULTS AND DISCUSSION

The electronic structure of α- and γ-Al_2O_3 was calculated using the free QUANTUM-ESPRESSO program package. The program is based on the density functional theory (DFT) with a plane-wave basis set and pseudopotentials approximation. We employed the ultrasoft pseudopotentials with the local density approximation and generalized gradient approximation. We used a periodic supercell approach for the simulation of the oxygen vacancy in α-Al_2O_3 and γ-Al_2O_3.

The perfect crystal of α-Al_2O_3 has a trigonal unit cell containing two Al_2O_3 molecules. The coordinates of the atoms are such that each Al atom is surrounded by six O atoms of two different nearest-neighbor (NN) distances and each O atom has four NN Al atoms. The γ-Al_2O_3 unit cell derived from spinel contains 40 atoms and there are two cation vacancies at octahedral sites, which are the farthest from each other. It was constructed as proposed in Ref. 18. In the γ-Al_2O_3 structure, the coordination numbers for O atoms can

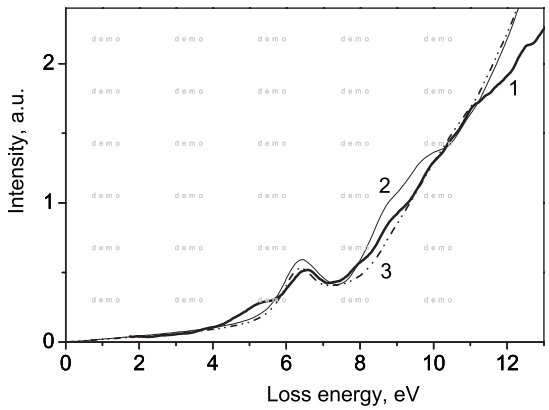

FIG. 1. Comparison of experimental EELS of amorphous Al_2O_3 recorded at E=50 eV (curve 1) with those calculated for α- and γ-Al_2O_3 with oxygen vacancies (2 and 3, respectively).

be either three or four, and the Al atoms can be fivefold or sixfold coordinated. For calculation of the defects in Al_2O_3, a supercell of sufficient size must be used in order to avoid the possible defect-defect interaction. The α- and γ-Al_2O_3 supercell contains a total of 160 atoms, in which one of the interior O atoms is removed to create an anion vacancy.

To study the electron/hole trapping by the defect, an extra electron was added/removed in the system with oxygen vacancy. The charge localization energies were estimated as difference between perfect and defect electron affinities and ionization energies as follows:[19]

$$\Delta\varepsilon^e = (E^{q=-1}_{perfect} - E^{q=0}_{perfect}) - (E^{q=-1}_{defect} - E^{q=0}_{defect});$$

$$\Delta\varepsilon^h = (E^{q=+1}_{perfect} - E^{q=0}_{perfect}) - (E^{q=+1}_{defect} - E^{q=0}_{defect}).$$

Figure 1 presents a comparison of the experimental EELS of amorphous Al_2O_3 with those calculated for α- and γ-Al_2O_3 with oxygen vacancy. The experimental EELS of amorphous Al_2O_3 contains an absorption peak at 6.5 eV, which is close to the well-known peak at 6.0 eV related to F center.[1–8] The theoretically calculated EEL spectra for α- and γ-Al_2O_3 cells with oxygen vacancies also show a peak at 6.4 eV, which is attributed to oxygen vacancy. Position of this peak is close to that in the experimental spectrum (Fig. 1, curve 1). These results show the presence of neutral oxygen vacancies in amorphous Al_2O_3 samples.

It has been established that the calculated absorption peak intensity decreases with reducing concentration of oxygen vacancies (i.e., increase in supercell size). Since experimental and calculated amplitudes nearly coincide, we can make a rough estimation of oxygen vacancy concentration in amorphous Al_2O_3. Our estimation gives a value of $N=7\times10^{20}$ cm^{-3}.

To identify oxygen vacancies independently, we recorded the low-temperature PL and PLE spectra of amorphous Al_2O_3. They are given in Figs. 2 and 3, respectively. As in the case of crystalline Al_2O_3, both PL and PLE spectra of amorphous Al_2O_3 demonstrate a set of broad bands: there is no fine structure even at liquid helium temperature. Thus, the case of strong electron-phonon interaction is realized and the Huang–Rhys factor values (S, average number of participating phonons) were estimated to be in the 9 to 12 range.[2,20] Such bands have the shape close to that of Gaussian and the result of their decomposition is given in Fig. 2(b).

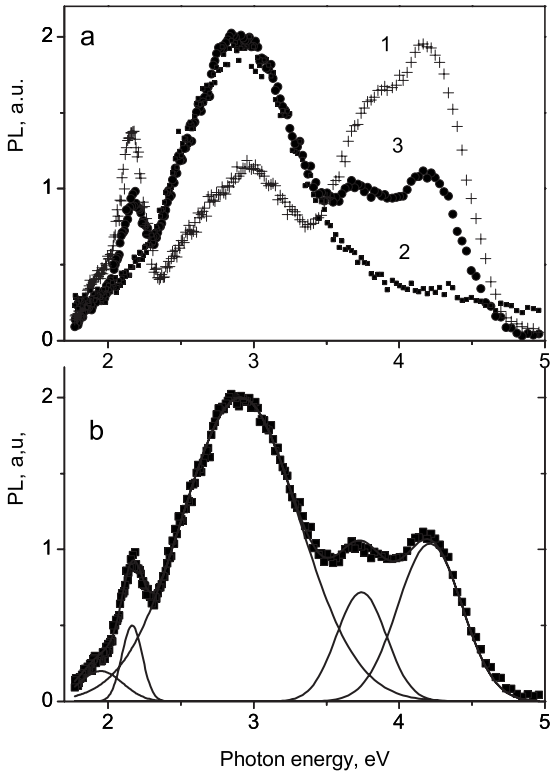

FIG. 2. (a) Time-resolved (1, 2) and time-integrated (3) PL spectra of amorphous Al_2O_3 under 6.52 eV excitation at 7.5 K. Spectra 1 and 2 present fast and slow components, respectively. (b) The time-integrated PL spectrum with results of its decomposition into Gaussian components.

In low-temperature PL spectra recorded at 6.52 eV excitation (Fig. 2), one can distinguish three main spectral ranges: 1.5–2.4, 2.5–3.4, and 3.5–4.8 eV. Slow emission component contains the only peak at 2.91 eV, which seems to have a low-energy shoulder. Fast emission component has additional peaks both at low-energy and high-energy sides. Result of time-integrated spectrum decomposition into Gaussian components is given in Fig. 2(b): maxima of additional peaks are located at 1.95, 2.165, 3.74, and 4.21 eV

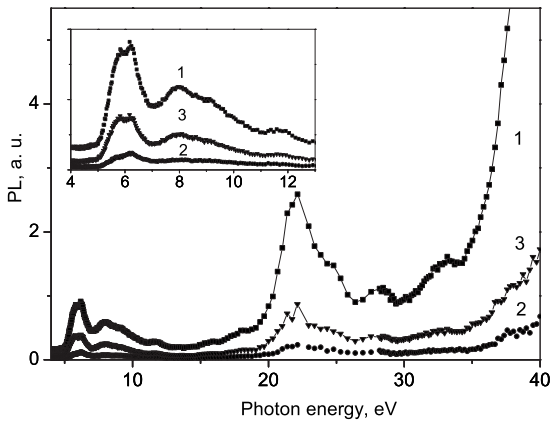

FIG. 3. Time-resolved (1, 2) and time-integrated (3) PLE spectra of luminescence in the 2.9 eV band of amorphous Al_2O_3. Spectra 1 and 2 present fast and slow components, respectively. Spectra were recorded at 7.5 K.

whereas their full width at half maximum values are 0.35 eV, 0.17 eV, 0.40 eV, and 0.52 eV, respectively. As follows from time-resolved measurements the PL decay time is short (~several nanoseconds) for these four last components, whereas that of the 2.91 eV component is much longer (tens of nanoseconds). All these PL transitions have been observed earlier in bulk α-Al_2O_3 samples and are related to intrinsic defects: they can be created only by corpuscular irradiation and thermochemical treatment, but not by the introduction of impurities.[1–8,21] Thus the slow PL component at 3.0 eV with a low-energy shoulder in bulk α-Al_2O_3 was related to neutral oxygen vacancy (F-center) (Refs. 2 and 8) whereas the fast 3.8 eV component was attributed to the same center but positively charged (F^+).[2,7] Corresponding peaks for amorphous Al_2O_3 films are located at 2.91 eV and 3.74 eV, respectively. What about the low-energy components at 1.95 and 2.165 eV, they can be due to some sort of pair centers (F_2-type centers) or interstitial cations.[21] The optical transitions of free Al^0, Al^+, and Al^{2+} are located in the 3 to 7.5 eV region but are shifted to lower energies when ions are incorporated into the Al_2O_3 structure.[21]

The PLE spectra for the 2.91 eV emission recorded in time-resolved and time-integrated regimes are shown in Fig. 3. One can see that the 2.91 eV luminescence of F-center in amorphous Al_2O_3 is effectively excited in three main ranges: 5–7, 7–13, and 20–26 eV. The PLE spectra recorded in different regimes (time-resolved and time-integrated ones) are similar to those for crystalline Al_2O_3.[8,19] The first range corresponds to intracenter excitation in oxygen vacancies, the second one is an excitation at the fundamental absorption edge ($h\nu \approx E_g$). These two ranges are shown in detail in the inset. The third range demonstrates the multiplication of electronic excitation at photon energy $h\nu \geq 2E_g$.

One can see that there are two well-pronounced maxima at 5.8 and 6.2 eV in the first range (Fig. 3, inset) and three ones at 7.98, 9.14, and 11.6 eV in the second range. The envelopes of PLE spectra for F-center emission in amorphous Al_2O_3 film (Fig. 3) and crystalline α-Al_2O_3 (Refs. 8 and 20) are similar enough. The main components in the low-energy range are centered at 5.6 and 6.3 eV for crystalline α-Al_2O_3 and their input depends considerably on light polarization and sample orientation.[8] This split is a result of excited state splitting in the crystal field of C_2 symmetry for the neutral vacancy. In crystalline Al_2O_3, the 6.3 eV component has an analog in the photoconductivity[2] and exoemission[22] spectra. This means that the upper components of split excited state are located in the conduction band and excitation in this band results in ionization of oxygen vacancy with the loss of an electron. Thus, the 2.9 eV luminescence and the 5.8 and 6.2 eV PLE bands prove unambiguously the presence of neutral oxygen vacancies in amorphous Al_2O_3 films produced in the ALD process. The spectroscopic parameters of oxygen vacancy in PL and PLE spectra for crystalline α- and γ-Al_2O_3 were found to be similar and close to those for amorphous Al_2O_3.

It is noteworthy that maximum of the second range PLE band is located at about 9 eV for α-Al_2O_3,[19] whereas for amorphous Al_2O_3 it is shifted to 7.98 eV. Since this range is related to band-to-band transitions, such shift means that E_g becomes narrower for amorphous Al_2O_3.

The quantum chemical simulation showed that the electron capture on oxygen vacancy is an energetically favorable process both in α- and γ-Al_2O_3. The calculated energy gain is 0.7 eV for electron trap in α-Al_2O_3, whereas in γ-Al_2O_3 this value is 0.6 eV and 0.8 eV for threefold and fourfold coordinated oxygen vacancies, respectively. The experimentally determined thermal activation energy for amorphous Al_2O_3 is 1.5 eV.[13] One can see that this value exceeds twice the calculated gain for electron capturing. The discrepancy is likely to be due to the underestimation of the band gap, which is a well-known tendency of the DFT technique. The hole capture is also an energetically favorable process for oxygen vacancy: the gain is 2.9 eV for α-Al_2O_3 and 1.5 eV for both types of oxygen vacancies in γ-Al_2O_3. Thus, oxygen vacancy is able to capture not only a hole, but also an electron and to operate as an electron trap in the last case. Taking into account the similarity of vacancy spectroscopic parameters in crystalline and amorphous Al_2O_3, this conclusion is related to amorphous Al_2O_3 as well.

Investigation of charge transport in amorphous ALD-produced Al_2O_3 showed that conductivity is determined by electron traps with thermal activation energy of about 1.5 eV.[13] Our estimations suggest that oxygen vacancies can be electron traps in amorphous Al_2O_3 as well.

IV. CONCLUSIONS

Thus, the first principle quantum chemical simulation combined with the EELS and optical spectroscopy shows that oxygen vacancies have similar parameters in crystalline α-Al_2O_3, γ-Al_2O_3, and amorphous Al_2O_3. It was established that amorphous Al_2O_3 films synthesized by the ALD method are oxygen deficient and this feature should be taken into account when using them in electronic devices.

ACKNOWLEDGMENTS

This work was supported by the Siberian Branch of the Russian Academy of Sciences (Integration Grant No. 70) and by the Ministry of Science and Technology of the Republic Korea (National Program for Tera-Level Nanodevices). We would like to thank A. V. Shaposhnikov for helpful discussions.

[1] G. W. Arnold and D. W. Compton, Phys. Rev. Lett. **4**, 66 (1960).
[2] B. G. Draeger and G. P. Summers, Phys. Rev. B **19**, 1172 (1979).
[3] P. W. M. Jacobs and E. A. Kotomin, Phys. Rev. Lett. **69**, 1411 (1992).
[4] K. J. Caulfield, R. Cooper, and J. F. Boas, Phys. Rev. B **47**, 55 (1993).
[5] A. Stashans, E. Kotomin, and J.-L. Calais, Phys. Rev. B **49**, 14854 (1994).
[6] Y.-N. Xu, Z.-Q. Gu, X.-F. Zhong, and W. Y. Ching, Phys. Rev. B **56**, 7277 (1997).
[7] K. Matsunaga, T. Tanaka, T. Yamamoto, and Y. Ikuhara, Phys. Rev. B **68**, 085110 (2003).
[8] A. I. Surdo, V. S. Kortov, V. A. Pustovarov, and V. Yu. Yakovlev, Phys. Status Solidi C **2**, 527 (2005).
[9] A. I. Kingon, J.-P. Maria, and S. K. Streiffer, Nature (London) **406**, 1032 (2000).
[10] J. Robertson, Eur. Phys. J.: Appl. Phys. **28**, 265 (2004).
[11] V. A. Gritsenko, K. A. Nasyrov, Y. N. Novikov, A. L. Aseev, S. Y. Yoon, J.-W. Lee, E.-H. Lee, and C. W. Kim, Solid-State Electron. **47**, 1651 (2003).

[12]C.-H. Cheng and J. Y.-M. Lee, Appl. Phys. Lett. **91**, 192903 (2007).
[13]Y. N. Novikov, V. A. Gritsenko, and K. A. Nasyrov, Appl. Phys. Lett. **94**, 222904 (2009).
[14]H. Nishikawa, R. Nakamura, Y. Ohki, and Y. Hama, Phys. Rev. B **48**, 2968 (1993).
[15]C. Itoh, K. Tanimura, N. Itoh, and M. Itoh, Phys. Rev. B **39**, 11183 (1989).
[16]H. Nishikawa, E. Watanabe, D. Ito, and Y. Ohki, Phys. Rev. Lett. **72**, 2101 (1994).
[17]G. Zimmerer, Nucl. Instrum. Methods Phys. Res. A **308**, 178, (1991).
[18]G. Gutiérrez, A. Taga, and B. Johansson, Phys. Rev. B **65**, 012101 (2001).
[19]A. X. Chu and W. B. Fowler, Phys. Rev. B **41**, 5061 (1990).
[20]A. I. Surdo, V. S. Kortov, and V. A. Pustovarov, Radiat. Meas. **33**, 587 (2001).
[21]M. J. Springis and J. A. Valbis, Phys. Status Solidi B **123**, 335 (1984).
[22]V. S. Kortov, I. I. Mil'man, S. V. Nikiforov, and V. E. Pelenev, Phys. Solid State **45**, 1260 (2003).